Available online at www.jourcc.com

Journal homepage: www.JOURCC.com

Journal of Composites and Compounds

Effect of Cu-substitution on the microstructure and magnetic properties of Fe-15%Ni alloy prepared by mechanical alloying

AliAsghar Abouchenari [a], Mostafa Moradi [b]*

[a] *Materials Science and Engineering Department, Shahid Bahonar University, Kerman, Iran*
[b] *Department of Materials Science and Engineering, Sharif University of Technology, Tehran, Iran*

ABSTRACT

In this study, nanostructured $(Fe_{85}Ni_{15})_{100-x}Cu_x$ (x = 0, 0.5, 1.5, 3 and 5) powders were synthesized via mechanical alloying process. The obtained phases, microstructure, and magnetic properties of these alloys were studied by X-ray diffraction analysis (XRD), scanning electron microscopy (SEM), and vibration sample magnetometer (VSM). XRD results indicated that after a suitable time of milling, Ni and Cu were homogeneously distributed in the Fe matrix, and (bcc) α-(Fe(Ni-Cu)) solid solution was obtained. It was found that by increasing Cu content in the alloy, work hardening increased, and thus the size of grains decreased while the internal micro-strain increased. Also, morphological observations indicated that the addition of Cu led to the formation of finer particles. Also, VSM analysis showed that the addition of Cu into Fe-Ni alloys lowered Ms. On the other hand, the coercivity increased by increasing copper content up to 1.5 at. %.

Peer review under responsibility of JCC Research Group.

ARTICLE INFORMATION

Article history:
Received 13 September 2019
Received in revised form 25 October 2019
Accepted 3 November 2019

Keywords:
Nano-crystalline alloys
Mechanical alloying
Ball mill
Fe-Ni-Cu alloy
Magnetic properties

1. Introduction

Recently, nanostructured materials have attracted great attention due to their excellent and unique electrical, magnetic, optical, catalytic, mechanical, and biological properties for various applications [1-11]. Several techniques including electrodeposition, rapid solidification [12-14], gas condensation, solid-state processing like friction stir welding (FSW) and mechanical alloying (MA) have been utilized to make nanostructured materials [15].

Among various techniques for fabricating such materials [16-19], it has been found that the solid state processing have some advantages in comparison with the convectional casting or rapid solidification methods [20-23]. This method, as a solid-state and non-equilibrium technique, is capable of producing a wide range of microstructures containing nano-crystalline supersaturated solid solutions, quasi-crystalline intermediates and amorphous phases [15, 20, 21, 24]. Also, in contrast to other new techniques such as liquid quenching (or melt-spinning), the MA process is a controllable process and operates at low temperatures as well as having the capability of large scale production [25-30].

During the first stages of the MA process, the impression force of the balls can deform the powder particles plastically and create new surfaces allowing the particles to bond together and thus results in an increment in the size of the particle [31]. For hard powders like nanosilica, the FSW method could be used for the production of composite-based nanostructures [32], but for ductile powders that tend to agglomerate, the ball mill acts better than FSW. Therefore, a wide range of particle sizes develops and the composite particles have a layered structure containing blends of the starting constituents. Further deformation, leads to strain hardening and hence fracture of particles by a fragmentation of fragile flakes and\or fatigue failure [33-36]. It is estimated that in the first few minutes up to an hour, the lamellar spaces typically become small and the crystallite size becomes nano-sized. After milling for a while, steady-state balance is obtained, between the rates of the welding and fracturing, at the same time because of the accumulation of strain energy, the particles reach a maximum hardness [20, 37]. As a result of the increased amount of cold working, the number of crystal defects (dislocation, vacancies, grain boundaries, stacking faults, etc.) increases with time and thus diffusivity of solute elements increases [38]. This leads to an increment in the defects and dislocations density which reduces the activation energy for diffusion. Hence, cold weld and fracture recurrence of powders in MA process make diffusion easier [39].

Iron is a good ferromagnetic material with a low resistivity that leads to large eddy current loss [40]. In addition, Fe-based nano-crystalline materials exhibit very suitable soft magnetic properties [41, 42], as well as high magnetization and low coercivity [43]. This makes them good candidates for several applications like magnetic sensors, magnetic clutches, magnetic shielding, etc. [44].

Magnetic iron-nickel alloys, generally called permalloys, are of excessive attention due to their magnetic properties, which makes them good candidates for use in automotive and nano-magnetic sensors [45-

* *Corresponding author: AliAsghar Abouchenari; E-mail: aliab596@yahoo.com*
DOR: 20.1001.1.26765837.2019.1.1.2.1
https://doi.org/10.29252/jcc.1.1.2

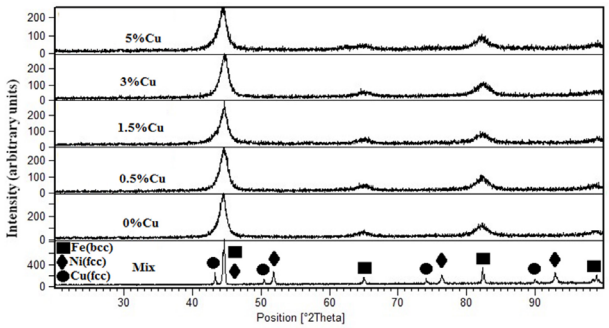

Fig. 1. X-ray diffraction pattern of (a) powder mixture before milling and after 72 h milling (b) FNC (c) FNC0.5 (d) FNC1.5 (d) FNC3 (e) FNC5.

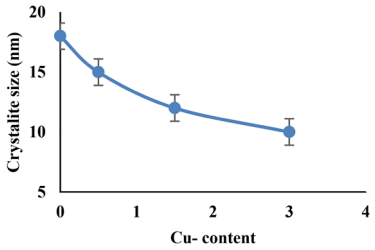

Fig. 2. Crystallite size as a function of copper content after milling for 72 h.

47].

Also, it is reported that a small amount of copper to Fe-Co alloys, leads to the grain size decrease and recovers some of the most important soft magnetic properties. Although there are several studies about the addition of various elements to Fe-Ni alloys, there is no report about the addition of Cu to this system. Accordingly, the aim of the present work is to investigate the effect of Cu doping on the microstructural and magnetic properties of nanocrystalline $Fe_{85}Ni_{15}$ alloys.

2. Materials and methods

In this study, Fe, Ni, and Cu powders with an average particle size of 15 μm, 10 μm and 63 μm, respectively, were supplied from Merck Co. The purity of Fe, Ni and Cu powders was 99.5%, 99.9% and 99.9%, respectively.

Firstly, the steel vials of the ball mill were loaded with special amounts of powders, in which the ball to powder weight ratio was about 20:1. Two kinds of stainless steel balls with a diameter of 20 and 10 mm were used to increase the welding and fracturing processes [48] and prevent the formation of the close-packed array [20].

The powders were mechanically alloyed in an inert (argon) atmosphere through a planetary ball mill (Fritsch, Pulverisette 4). Common milling speed of 350 rpm and milling time of 72 h was employed. Five samples of $(Fe_{85}Ni_{15})_{100-x}Cu_x$ (x = 0, 0.5, 1.5, 3 and 5) system were prepared with different copper contents (Table 1).

The milled powders were characterized by X-ray diffraction analysis (XRD), which was carried out by a Philips X'pert High Score diffractometer (Brukers D8 System Germany) using Cu kα (λ = 0.1542 nm). For all the XRD investigations, an angular range (2θ) of 20° – 90° was used. The crystallite size and the internal strain were determined by the Williamson- Hall method (Eq. 1) as below [49, 50]:

$$\beta cos\theta = 2\varepsilon sin\theta + 0.9\frac{\lambda}{D} \quad (1)$$

where is the full-width at half-maximum (FWHM) of a diffraction peak, θ is the Bragg angle, D is the grain size, ε is the lattice strain, and λ is the X-ray wavelength [51, 52]. The XRD peaks were fitted by four-variable Gaussian functions using the sigma plot V.12.0 software. β can be determined as follows (Eq. 2):

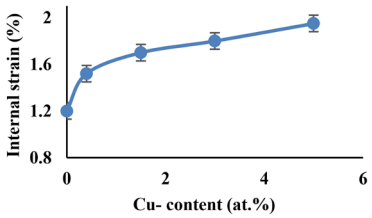

Fig. 3. Lattice strain change after 72 h milling for the samples with different contents of Cu.

$$\beta^2 = \beta_m^2 - \beta_c^2 \quad (2)$$

where β_c is the instrument broadening and β_m is the measured half-width broadening.

The morphology, microstructure and particles size of the powder were obtained by scanning electron microscopy (SEM) test via a Philips XL30 instrument. The mean particle size of about 350 particles was calculated by image analyzer software of Clemex version V 3.5. The magnetic properties of the milled powder were measured at room temperature by using vibrating sample magnetometer (VSM) at the maximum field of 10 kOe.

3. Results and discussion

3.1. Microstructure

Fig. 1 shows the X-ray diffraction patterns of the mixture of initial powders and mechanically alloyed samples after milling for 72 h. It can be seen that the XRD patterns of the samples before milling have only the peaks corresponded to Fe, Ni, and Cu elements. On the other hand, after 72 h milling, there was no trace of Ni and Cu peaks in the XRD patterns. Reactions finished in the vial before milling completion and the final product was 100% solid solution of α-Fe(Ni-Cu). Since the atomic diffusion is time-dependent, sufficient milling time is required to obtain the final products. By increasing the Cu content, the diffraction peaks became broader and less intense. This represents the continuous decrease in the crystallite size and the introduction of lattice strain.

This broadening is due to the second-order internal stress that affects the crystals at the macroscopic level and leads to the broadening of diffraction peaks [53, 54]. Also, the decrease in peak intensity can be attributed to different lattice parameters of Ni and Cu, i.e., the solid solution is formed [55] and induced strain is caused by the plastic deformation [56]. After milling for 72 hours and subsequent increase in the Cu content, it was observed that the peak corresponding to the (110) phase alpha-Fe bcc, has been shifted towards lower angles. The reason is that by increasing the amount of copper, more copper is dissolved in the iron structure that leads to the change in lattice parameters. Also, the iron peaks are shifted toward lower angles which is due to the entrance of Ni and Cu atoms to the Fe structure that leads to formation of solid solutions of (Ni)-Fe and bcc Fe-(Ni, Cu). Kaloshkin et al. [57] showed that the milled alloy powder of Fe-10% Ni showed only the bcc phase. In addition, the slight shift may be caused by first-order internal stress at a macroscopic level by changing the lattice parameter [54, 58].

Table 1.
Different compositions of $(Fe_{85}Ni_{15})_{100-x}Cu_x$ system.

Sample	Cu content	Code
1	0	FNC
2	0.5	FNC0.5
3	1.5	FNC1.5
4	3	FNC3
5	5	FNC5

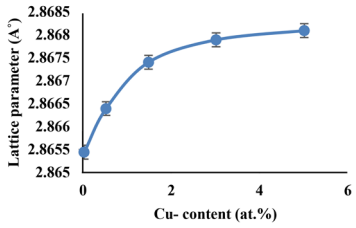

Fig. 4. Variation of lattice parameter after 72 h milling of samples with different contents of Cu.

Repeated fracture and welding of particles having large contact surfaces are reduced at ambient temperature, which leads to the formation of solid-solution during the mechanical alloying [56]. Moreover, the density of defects increased during the severe deformation while the diffusion distance decreased which provides suitable diffusion paths for Ni and Cu atoms in the iron lattice [20, 59].

Fig. 2 represents the effect of copper content on the crystallite size of milled alloys. It can be noticed that by increasing Cu content, the crystallite size of alloys decreased from 18 to 8 nm. This can be related to the solubility of Cu atoms in the iron structure and its hardening effect. Smaller crystallite size would lead to higher strength and hardness [60].

It can also reduce the grain size of powders that occurs during severe plastic deformation that results in strain hardening [61, 62] [63]. Hamzaoui et al. [64] showed that by adding 10% nickel to iron, its crystallite size decreased to 10.4 nm after milling for 96 h. At the first stages of MA, a great amount of crystal defects e.g. dislocations are created. At longer milling time, higher dislocation density is formed which might lead to the formation of new boundaries inside nanoscale crystals [65].

Fig. 3 demonstrates the internal strain variation of Fe-(Ni, Cu) structure for different Cu contents after 72 h milling. As it is illustrated, by increasing the amount of copper content, a great increase was observed in the rate of internal strain at first but, at 1.5 at. % Cu, the amount of internal strain became a plateau.

Generally, the increase in micro-strain value might be due to the severely cold working and plastic deformation of powders. Commonly, during mechanical alloying defects are formed in the interface of grains [60, 66-69]. The increase in strain level has corresponded to high dislocations' density [70].

The volume fraction of grain boundaries (f_{gb}) in polycrystalline materials can be estimated as below:

$$f_{gb} = 1 - f_g \quad (3)$$

where f_g is the grain volume fraction given by:

$$f_g = \frac{(D-d)^3}{D^3} \quad (4)$$

where D represents crystallite size and d is the effective thickness of the grain boundary [65, 71, 72].

Table 2.
The volume fraction of grain boundaries for the samples with various contents of copper.

Sample	D (nm)	F_{gb} (%)
FNC	18	12
FNC0.5	15	14
FNC1.5	12	18
FNC3	10	21
FNC5	8	26

Table 2 lists the changes in grain boundaries' volume fraction versus Cu content after 72 h milling. From table 2, it is obvious that as the copper content increased, the crystallite size decreased while f_{gb} increased. This is because of the grain boundaries' effect on the movement of dislocations.

Fig. 4 shows the variation of the lattice parameter (ao) with different copper contents after 72 h milling. According to the figure, the lattice parameter increased by increasing Cu content and reached a plateau at 5 %. This can be due to the saturation of Cu atoms in the Fe structure. Furthermore, the lattice expansion could be attributed to the dissolution of copper with a higher radius into the interstitial sites [73]. However, it could be due to the severe plastic deformation of the powders during MA [74], in which the dislocations are formed as well as sub-boundaries. This leads to faster diffusion of Cu into the Fe structure. Accordingly, during the mechanical alloying operation, lattice parameter difference, and concentration of defects such as dislocations and vacancies, result in an increment in the lattice parameter [68].

3.2. Morphology and Particle Size

Fig. 5 depicts the SEM micrographs of powder of all samples after 72 h milling. The relating average particle size of the powders is shown in Fig. 6. Accordingly, by increasing the content of copper, the average particle size decreased. The minimum average particle size was obtained about 3 µm for 5 at. % of Cu. Powders became finer and particle size distribution was uniform with spherical and equal size shapes. It can be seen that the MA processing time was high enough to decrease the particle size distribution. Also, the powder had an almost spherical shape and the addition of Cu makes the particles more brittle which may cause higher grinding of powder and finer particles.

3.3. Magnetic properties

3.3.1. Saturation Magnetization

Fig. 7 depicts the variations of saturation magnetization after 72 h,

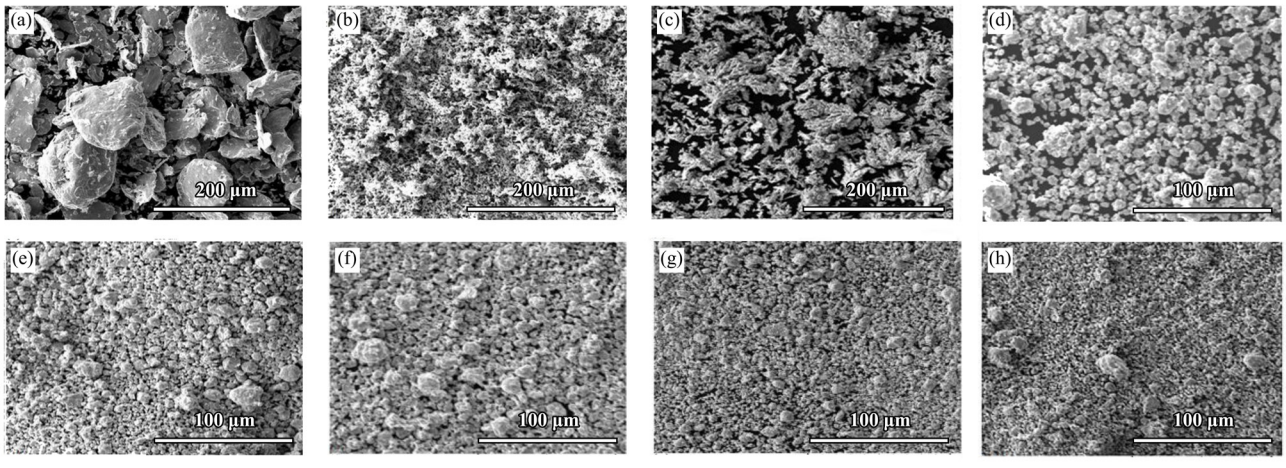

Fig. 5. SEM images of powders milled for 72 h containing (a) 0, (b) 1.5, (c) 3, and (d) 5 at.% Cu.

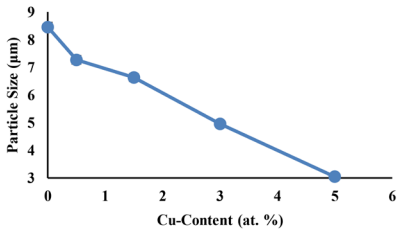

Fig. 6. Average particle size of the powders for samples with different amounts of Cu after 72 h milling.

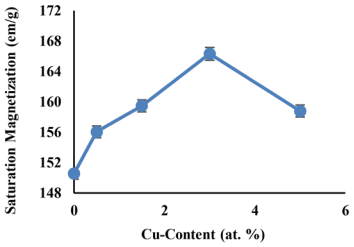

Fig. 7. Saturation magnetization changes after 72 h milling for the samples with different contents of Cu.

for the milled samples with different contents of copper. It can be seen that the magnetization decreases slightly with increasing the Cu content that can be attributed to the diamagnetic nature of Cu in the structure [65, 75]. The introduction of diamagnetic moments into the specimens leads to the decrease in magnetic properties during the milling process [76] that would be due to the movement of domain walls [75] which can be affected by the defects induced by milling and can greatly hinder the wall movement through the defects. The decrease of crystallite size during the microstructure refinement leads to an increment in grain boundary volume fraction which, in turn, causes an increase in the amount of the atoms present in the grain boundary.

This is because of the low density of grain boundaries structure and higher interatomic distances between neighbor atoms that can decrease the effective magnetic moment by variation of the magnetic exchange interaction of the nearest atoms [77, 78]. On the other hand, due to the change in lattice parameter, the addition of copper leads to a remarkable expansion in the Fe lattice, i.e., the expansion of the lattice has a significant effect on the distance between atoms that are associated with a severe decrease in the saturation magnetization [79]. Slight increase of M_s can be due to the dominance of nanostructure effect over the negative effect of copper. Also, it can be attributed to the presence of surrounding Ni on Fe atoms. Furthermore, this can be corresponded to increment in contamination level due to long milling time [49] as well as the formation of defects that may negatively affect the ferromagnetic ordering [68].

3.3.2. Coercivity

Fig. 8 shows the variation of coercivity with different contents of copper after milling for 72 h. According to the figure, the coercivity first increased by increasing the Cu content, up to 1.5% (61.28 Oe), and then decreased to 32.26 Oe. The initial increment of the coercivity could be due to several factors such as higher residual stress and dislocation density as a result of the severe plastic deformation through milling.

During the milling process, impurities and contaminations such as oxides are transferred from container to the powder. These non-magnetic impurities can increase the H_c since they are the main factor in closing the magnetic domain walls [80].

Accordingly, it was observed that by increasing the percentage of copper up to 3%, the coercivity rapidly reduced. The relationship between H_c, M_s, and grain size is as follows [25, 65]:

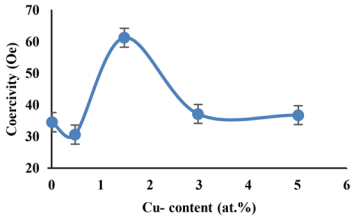

Fig. 8. Variation of coercivity for samples with different contents of Cu.

$$H_C \approx 3\sqrt{\frac{kT_C K_1}{aM_S}}\frac{1}{D} \quad (5)$$

in which, D, K_1, T_c, and k are the crystallite size, magnetic-crystalline anisotropy, Corie temperature, respectively, and k is constant [81].

According to obtained results, at lower contents of 3% Cu, the grains size (12 nm) is more than the exchange length (L_{ex}). When the grains size is more than L_{ex}, the grains boundary hinders the field wall, since volume fraction of grain boundaries increases as a result of grains fining. When crystallite size (10 nm) is less than exchange length, effect of the field walls decreases and each grain acts as a separate filed. In this case, there is no grain boundary, therefore, magnetic walls move easier and H_c decreases.

4. Conclusions

The nanocrystalline $(Fe_{85}Ni_{15})_{100-x}Cu_x$ (x=0, 0.5, 1.5, 3, and 5) system was successfully prepared through the mechanical alloying method. Increasing copper content enhanced the rate of hard-working which leads to an increment in defects especially dislocations. This led to the reduction of crystallite size as well as the increment of internal strain. The X-ray diffraction peaks were broadened with increasing copper content, which mainly was due to decreased crystallite size and increased lattice strain. The crystallite size varied in the range of 18 to 8 nm in copper-free Fe-Ni up to 5% Cu content. Also, the lattice parameter was higher in copper-containing samples. The addition of Cu into Fe-Ni alloys lowered the M_s, which was due to its diamagnetic effect. On the other hand, the coercivity increased by increasing copper content up to 1.5%. This was due to the increment in crystal defects and finer grain size.

Acknowledgments

The authors thank the University of Shahid Bahonar, Kerman, Iran, for its financial and other support

Conflict of Interest

All authors declare no conflicts of interest in this paper..

REFERENCES

[1] I. Capek, Nanocomposite Structures and Dispersions, Elsevier Science, USA, 2006.

[2] S. Miraghaei, P. Abachi, H. Madaah-Hosseini, A. Bahrami, Characterization of mechanically alloyed Fe100−xSix and Fe83.5Si13.5Nb3 nanocrystalline powders, journal of materials processing technology 203(1-3) (2008) 554-560.

[3] J. Jeevanandam, A. Barhoum, Y.S. Chan, A. Dufresne, M.K. Danquah, Review on nanoparticles and nanostructured materials: history, sources, toxicity and regu-lations, Beilstein journal of nanotechnology 9(1) (2018) 1050-1074.

[4] M.S. Leila Bazli, Arman Shiravi, A Review of Carbon nanotube/TiO2 Compos-ite prepared via Sol-Gel method Composites and Compounds 1(1) (2019) 1-12.

[5] M. Radmansouri, E. Bahmani, E. Sarikhani, K. Rahmani, F. Sharifianjazi, M. Irani, Doxorubicin hydrochloride-Loaded electrospun chitosan/cobalt ferrite/tita-nium oxide nanofibers for hyperthermic tumor cell treatment and controlled drug release, International journal of biological macromolecules 116 (2018) 378-

384.
[6] V. Balouchi, F.S. Jazi, A. Saidi, Developing (W, Ti) C-(Ni, Co) nanocomposite by SHS method, Journal of Ceramic Processing Research 16(5) (2015) 605-608.
[7] A. Masoudian, M. Karbasi, F. SharifianJazi, A. Saidi, Developing Al2O3-TiC in-situ nanocomposite by SHS and analyzingtheeffects of Al content and mechanical activation on microstructure, Journal of Ceramic Processing Research 14(4) (2013) 486-491.
[8] F. Sharifianjazi, N. Parvin, M. Tahriri, Formation of apatite nano-needles on novel gel derived SiO2-P2O5-CaO-SrO-Ag2O bioactive glasses, Ceramics Interna-tional 43(17) (2017) 15214-15220.
[9] Z.B. Jiao, J.H. Luan, M.K. Miller, C.Y. Yu, C.T. Liu, Group precipitation and age hardening of nanostructured Fe-based alloys with ultra-high strengths, scientific reports 6 (2016) 21364.
[10] X. Xu, F. Song, X. Hu, A nickel iron diselenide-derived efficient oxygen-evo-lution catalyst, Nature Communications 7(1) (2016) 12324.
[11] M. Habibi Jouybari, S. Hosseini, K. Mahboobnia, L.A. Boloursaz, M. Moradi, M. Irani, Simultaneous controlled release of 5-FU, DOX and PTX from chitosan/PLA/5-FU/g-C3N4-DOX/g-C3N4-PTX triaxial nanofibers for breast cancer treatment in vitro, Colloids and Surfaces B: Biointerfaces 179 (2019) 495-504.
[12] D.M. Matson, Retained free energy as a driving force for phase transformation during rapid solidification of stainless steel alloys in microgravity, npj Micrograv-ity 4(1) (2018) 22.
[13] F. He, Z. Wang, Y. Li, Q. Wu, J. Li, J. Wang, C.T. Liu, Kinetic ways of tailor-ing phases in high entropy alloys, Scientific Reports 6 (2016) 34628.
[14] K.J. Dusoe, S. Vijayan, T.R. Bissell, J. Chen, J.E. Morley, L. Valencia, A.M. Dongare, M. Aindow, S.-W. Lee, Strong, ductile, and thermally stable Cu-based metal-intermetallic nanostructured composites, Scientific Reports 7(1) (2017) 40409.
[15] C. Koch, Top-down synthesis of nanostructured materials: Mechanical and thermal processing methods, Reviews on Advanced Materials Science 5(2) (2003) 91-99.
[16] K. Akkouche, A. Guittoum, N. Boukherroub, N. Souami, Evolution of structure, microstructure and hyperfine properties of nanocrystalline Fe50Co50 powders prepared by mechanical alloying, Journal of Magnetism and Magnetic Materials 323(21) (2011) 2542-2548.
[17] M.A. Meyers, A. Mishra, D.J. Benson, Mechanical properties of nanocrystal-line materials, Progress in materials science 51(4) (2006) 427-556.
[18] B. Zuo, T. Sritharan, Ordering and grain growth in nanocrystalline Fe75Si-25alloy, Acta Materialia 53(4) (2005) 1233-1239.
[19] R.B. Azhiri, R. Mehdizad Tekiyeh, E. Zeynali, M. Ahmadnia, F. Javidpour, Measurement and evaluation of joint properties in friction stir welding of ABS sheets reinforced by nanosilica addition, Measurement 127 (2018) 198-204.
[20] C. Suryanarayana, Mechanical alloying and milling, Progress in materials science 46(1-2) (2001) 1-184.
[21] C. Suryanarayana, Inoue, A, Bulk Metallic Glasses, 2nd ed., CRC Press (2018).
[22] M.-L. Cui, Y.-S. Chen, Q.-F. Xie, D.-P. Yang, M.-Y. Han, Synthesis, properties and applications of noble metal iridium nanomaterials, Coordination Chemistry Reviews 387 (2019) 450-462.
[23] Z.-G. Wang, J.-H. Ouyang, Y.-J. Wang, L.-Y. Xie, Y.-H. Ma, Z.-G. Liu, A. Henniche, Y. Wang, Microstructural characterization of nanostructured Al2O3-ZrO2eutectic layer by laser rapid solidification method, Applied Surface Science 476 (2019) 335-341.
[24] A. Rostami, G.A. Bagheri, S.K. Sadrnezhaad, Microstructure and thermody-namic investigation of NiTi system produced by mechanical alloying, Physica B: Condensed Matter 552 (2019) 214-220.
[25] T. Sourmail, Near equiatomic FeCo alloys: constitution, mechanical and mag-netic properties, Progress in Materials Science 50(7) (2005) 816-880.
[26] L. Nath, G.C. Saha, R. Brüning, Nanocrystalline Al2O3-Ni(Cr) particle synthe-sis by high-energy mechanical alloying method, Journal of Alloys and Compounds 758 (2018) 224-236.
[27] A. Esmaeilkhanian, F. Sharifianjazi, A. Abouchenari, A. Rouhani, N. Parvin, M. Irani, Synthesis and Characterization of Natural Nano-hydroxyapatite Derived from Turkey Femur-Bone Waste, Applied Biochemistry and Biotechnology 189(3) (2019) 919-932.
[28] A. Moghanian, F. Sharifianjazi, P. Abachi, E. Sadeghi, H. Jafarikhorami, A. Sedghi, Production and properties of Cu/TiO2 nano-composites, Journal of Alloys and Compounds 698 (2017) 518-524.
[29] E.H. Jazi, R. Esalmi-Farsani, G. Borhani, F.S. Jazi, Synthesis and Character-ization of In Situ Al-Al13Fe4-Al2O3-TiB2 Nanocomposite Powder by Mechanical Alloying and Subsequent Heat Treatment, Synthesis and Reactivity in Inorganic, Metal-Organic, and Nano-Metal Chemistry 44(2) (2014) 177-184.
[30] M. Alizadeh, F. Sharifianjazi, E. Haghshenasjazi, M. Aghakhani, L. Rajabi, Production of nanosized boron oxide powder by high-energy ball milling, Synthe-sis and Reactivity in Inorganic, Metal-Organic, and Nano-Metal Chemistry 45(1) (2015) 11-14.
[31] A.S. Wismogroho, W.B. Widayatno, M.I. Amal, Y. Affandi, G.S.T. Sinaga, A. Fitroturokhmah, R. Kusumaningrum, Microstructure transformation of Cr-Al-BN coating on low carbon steel prepared by ball milling method, IOP Conference Series: Materials Science and Engineering 478 (2019) 012004.
[32] R.B. Azhiri, J.F. Sola, R.M. Tekiyeh, F. Javidpour, A.S. Bideskan, Analyzing of joint strength, impact energy, and angular distortion of the ABS friction stir welded joints reinforced by nanosilica addition, The International Journal of Advanced Manufacturing Technology 100(9) (2019) 2269-2282.
[33] W.L. Johnson, Thermodynamic and kinetic aspects of the crystal to glass transformation in metallic materials, Progress in Materials Science 30(2) (1986) 81-134.
[34] C.C. Koch, Processing of metals and alloys, Materials Science and Technology-A Comprehensive Treatment 15 (1991) 193-245.
[35] M. Oehring, Z.H. Yan, T. Klassen, R. Bormann, Competition between stable and metastable phases during mechanical alloying and ball milling, physica status solidi (a) 131(2) (1992) 671-689.
[36] C.C. Koch, Structural nanocrystalline materials: an overview, Journal of Ma-terials Science 42(5) (2007) 1403-1414.
[37] A. Abu-Oqail, A. Wagih, A. Fathy, O. Elkady, A.M. Kabeel, Effect of high energy ball milling on strengthening of Cu-ZrO2 nanocomposites, Ceramics Inter-national 45(5) (2019) 5866-5875.
[38] Y. Afkham, R.A. Khosroshahi, R. Taherzadeh Mousavian, D. Brabazon, R. Kheirifard, Microstructural characterization of ball-milled metal matrix nanocom-posites (Cr, Ni, Ti)-25 wt% (Al2O3np, SiCnp), Particulate Science and Technology 36(1) (2018) 72-83.
[39] L. Lu, M.O. Lai, Formation of new materials in the solid state by mechanical alloying, Materials & Design 16(1) (1995) 33-39.
[40] M.D. Chermahini, S. Sharafi, H. Shokrollahi, M. Zandrahimi, Microstructural and magnetic properties of nanostructured Fe and Fe50Co50 powders prepared by mechanical alloying, Journal of Alloys and Compounds 474(1-2) (2009) 18-22.
[41] V. Chaudhary, X. Chen, R.V. Ramanujan, Iron and manganese based magnetocaloric materials for near room temperature thermal management, Progress in Materials Science 100 (2019) 64-98.
[42] A.R. Rouhani, A.H. Esmaeil-Khanian, F. Davar, S. Hasani, The effect of agarose content on the morphology, phase evolution, and magnetic properties of CoFe2O4 nanoparticles prepared by sol-gel autocombustion method, International Journal of Applied Ceramic Technology 15(3) (2018) 758-765.
[43] A.H. Taghvaei, A. Ebrahimi, M. Ghaffari, K. Janghorban, Investigating the magnetic properties of soft magnetic composites based on mechanically alloyed nanocrystalline Fe–5 wt% Ni powders, Journal of Magnetism and Magnetic Mate-rials 323(1) (2011) 149-155.
[44] A. Inoue, T. Zhang, W. Zhang, A. Takeuchi, Bulk Nd–Fe–Al amorphous alloys with hard magnetic properties, Materials Transactions, JIM 37(2) (1996) 99-108.
[46] Magnetic neutron scattering, in: Y. Zhu (Ed.), Modern Techniques for Characterizing Magnetic Materials, Springer US, Boston, MA, 2005, pp. 3-64.
[46] A. Rathi, V.M. Meka, T.V. Jayaraman, Synthesis of nanocrystalline equiatom-ic nickel-cobalt-iron alloy powders by mechanical alloying and their structural and magnetic characterization, Journal of Magnetism and Magnetic Materials 469 (2019) 467-482.
[47] M. Wack, M. Volk, Q. Wei, Magnetic Properties of the Iron–Nickel System: Pressure, Composition, and Grain Size, in: H. Lühr, J. Wicht, S.A. Gilder, M. Holschneider (Eds.), Magnetic Fields in the Solar System: Planets, Moons and Solar Wind Interactions, Springer International Publishing, Cham, 2018, pp. 383-406.
[48] P. Soni, Mechanical alloying: fundamentals and applications, Cambridge Int Science Publishing2000.
[49] B.D. Cullity, Elements of X-ray diffraction, Addison, Wesley Mass (1978).
[50] G. Williamson, W. Hall, X-ray line broadening from filed aluminium and wolfram, Acta metallurgica 1(1) (1953) 22-31.
[51] S. Takaki, F. Jiang, T. Masumura, T. Tsuchiyama, Correction of Elastic An-isotropy in Williamson-Hall Plots by Diffraction Young's Modulus and Direct Fitting Method, ISIJ International 58(4) (2018) 769-775.
[52] A. Khorsand Zak, W.H. Abd. Majid, M.E. Abrishami, R. Yousefi, X-ray analysis of ZnO nanoparticles by Williamson–Hall and size–strain plot methods, Solid State Sciences 13(1) (2011) 251-256.
[53] L. Castex, J.-L. Lebrun, G. Maeder, J.-M. Sprauel, Détermination des con-traintes résiduelles par diffraction des rayons X, ENSAM1981.
[54] A. Guittoum, A. Layadi, A. Bourzami, H. Tafat, N. Souami, S. Boutarfaia, D. Lacour, X-ray diffraction, microstructure, Mössbauer and magnetization studies of

nanostructured Fe50Ni50 alloy prepared by mechanical alloying, Journal of Magnetism and Magnetic Materials 320(7) (2008) 1385-1392.
[55] H.R. Madaah Hosseini, A. Bahrami, Preparation of nanocrystalline Fe–Si–Ni soft magnetic powders by mechanical alloying, Materials Science and Engineer-ing: B 123(1) (2005) 74-79.
[56] T.T. Saravanan, S. Kumaran, T.S. Rao, Structural evolution and magnetic properties of mechanically alloyed metastable Fe–Ni–Zr–B system, Materials Letters 63(9) (2009) 780-782.
[57] S.D. Kaloshkin, V.V. Tcherdyntsev, I.A. Tomilin, Y.V. Baldokhin, E.V. Shelekhov, Phase transformations in Fe–Ni system at mechanical alloying and consequent annealing of elemental powder mixtures, Physica B: Condensed Matter 299(3) (2001) 236-241.
[58] A. Djekoun, B. Bouzabata, A. Otmani, J.M. Greneche, X-ray diffraction and Mössbauer studies of nanocrystalline Fe-Ni alloys prepared by mechanical alloy-ing, Catalysis Today 89(3) (2004) 319-323.
[59] D.A. Porter, K.E. Easterling, M. Sherif, Phase Transformations in Metals and Alloys, (Revised Reprint), CRC press2009.
[60] B. Bhoi, V. Srinivas, V. Singh, Evolution of microstructure and magnetic properties of nanocrystalline Fe70−xCuxCo30 alloy prepared by mechanical alloying, Journal of Alloys and Compounds 496(1-2) (2010) 423-428.
[61] J.R. Ares, F. Cuevas, A. Percheron-Guégan, Mechanical milling and subsequent annealing effects on the microstructural and hydrogenation properties of multisubstituted LaNi5 alloy, Acta Materialia 53(7) (2005) 2157-2167.
[62] A. Hossein Taghvaei, A. Ebrahimi, M. Ghaffari, K. Janghorban, Investigating the magnetic properties of soft magnetic composites based on mechanically alloyed nanocrystalline Fe–5wt% Ni powders, Journal of Magnetism and Magnetic Materials 323(1) (2011) 149-155.
[63] S.K. Vajpai, B.V. Mahesh, R.K. Dube, Studies on the bulk nanocrystalline Ni–Fe–Co alloy prepared by mechanical alloying–sintering–hot rolling route, Journal of Alloys and Compounds 476(1) (2009) 311-317.
[64] R. Hamzaoui, O. Elkedim, N. Fenineche, E. Gaffet, J. Craven, Structure and magnetic properties of nanocrystalline mechanically alloyed Fe–10% Ni and Fe–20% Ni, Materials Science and Engineering: A 360(1-2) (2003) 299-305.
[65] A.H. Bahrami, H. Ghayour, S. Sharafi, Evolution of microstructural and mag-netic properties of mechanically alloyed Fe80−xNi20Six nanostructured powders, Powder Technology 249 (2013) 7-14.
[66] D.L. Zhang, Processing of advanced materials using high-energy mechanical milling, Progress in Materials Science 49(3) (2004) 537-560.
[67] B. Bhoi, V. Srinivas, V. Singh, Evolution of microstructure and magnetic properties of nanocrystalline Fe70−xCuxCo30 alloy prepared by mechanical alloying, Journal of Alloys and Compounds 496(1) (2010) 423-428.
[68] M. Tavakoli, H. Shokrollahi, L. Karimi, K. Janghorban, Investigation of struc-tural, microstructural and magnetic properties of mechanically alloyed nanostruc-tured (Fe50Co50)100−xMox(x=25,35) powders, Powder Technology 234 (2013) 13-18.
[69] Y. Shen, H.H. Hng, J.T. Oh, Synthesis and characterization of high-energy ball milled Ni–15%Fe–5%Mo, Journal of Alloys and Compounds 379(1) (2004) 266-271.
[70] F.A. Mohamed, A dislocation model for the minimum grain size obtainable by milling, Acta Materialia 51(14) (2003) 4107-4119.
[71] B. Chitsazan, H. Shokrollahi, A. Behvandi, M. Ghaffari, Magnetic, structural and micro-structural properties of mechanically alloyed nano-structured Fe-48Co48V4 powder containing inter-metallic Co3V, Journal of Magnetism and Mag-netic Materials 323(9) (2011) 1128-1133.
[72] J.M. Greneche, A. Ślawska-Waniewska, About the interfacial zone in nano-crystalline alloys, Journal of Magnetism and Magnetic Materials 215-216 (2000) 264-267.
[73] S. Sharma, C. Suryanarayana, Effect of Nb on the glass-forming ability of me-chanically alloyed Fe–Ni–Zr–B alloys, Scripta Materialia 58(6) (2008) 508-511.
[74] J.J. Suñol, J.M. Güell, J. Bonastre, S. Alleg, Structural study of nanocrystal-line Fe–Co–Nb–B alloys prepared by mechanical alloying, Journal of Alloys and Compounds 483(1) (2009) 604-607.
[75] B.D. Cullity, C.D. Graham, Introduction to magnetic materials, John Wiley & Sons2011.
[76] T.D. Shen, R.B. Schwarz, J.D. Thompson, Soft magnetism in mechanically alloyed nanocrystalline materials, Physical Review B 72(1) (2005) 014431.
[77] M.P.C. Kalita, A. Perumal, A. Srinivasan, Structure and magnetic properties of nanocrystalline Fe75Si25 powders prepared by mechanical alloying, Journal of Magnetism and Magnetic Materials 320(21) (2008) 2780-2783.
[78] A. Antolak, D. Oleszak, M. Pękała, T. Kulik, Structure and magnetic properties of mechanically alloyed Ni–Ge and Co–Ge alloys, Materials Science and Engineering: A 449-451 (2007) 440-443.
[79] R. Besmel, H. Shokrollahi, Simultaneous variations of microstructure and magnetic properties of Ni58Fe12Zr20B10 nanostructure/amorphous alloy prepared by mechanical alloying, Journal of Magnetism and Magnetic Materials 324(18) (2012) 2829-2835.
[80] F. Bødker, S. Mørup, S. Linderoth, Surface effects in metallic iron nanoparticles, Physical Review Letters 72(2) (1994) 282-285.
[81] M.E. McHenry, M.A. Willard, D.E. Laughlin, Amorphous and nanocrystal-line materials for applications as soft magnets, Progress in materials Science 44(4) (1999) 291-433.